Solar Energy Materials & Solar Cells 287 (2025) 113603

Contents lists available at ScienceDirect

Solar Energy Materials and Solar Cells

journal homepage: www.elsevier.com/locate/solmat

# Less is more: Enabling low-filled electrically conductive adhesives for shingled solar cell interconnection using the capillary suspension concept

Marianne Kronsbein [a,*,1], Leonhard Böck [b,1], Katrin Dyhr [a,1], Torsten Rößler [b], Norbert Willenbacher [a]

[a] Karlsruhe Institute of Technology, Gotthard-Franz-Straße 3, 76131, Karlsruhe, Germany
[b] Fraunhofer Institute for Solar Energy Systems, Heidenhofstraße 2, 79110, Freiburg, Germany

ARTICLE INFO

*Keywords:*
Electrically conductive adhesives (ECA)
Low temperature
Silver saving
Capillary suspension
Shingling

ABSTRACT

Lead-free, low temperature materials for solar cell interconnection gain relevance in upcoming cell and module concepts. Electrically Conductive Adhesives (ECAs) are such materials but typically come with a high silver content. We herein give an overview on ECA requirements for shingled cell interconnection. Regular ECAs and stabilized ECAs with varying filler content were characterized regarding their rheological, curing, electrical and mechanical behaviour and their performance in modules. It was found that 20 vol% silver is necessary to meet the electrical requirements with a regular epoxy-based ECA containing micron-sized silver flakes. Regarding mechanical properties, as little filler as possible is favourable. To fulfil both the electrical and mechanical requirements, application of the capillary suspension concept to ECAs was found to be suitable. Such an ECA with only 5 vol% silver filler exhibits a volume and contact resistivity of (4.5 ± 0.5) $10^{-3}$ Ω cm and (0.026 ± 0.006) mΩ $cm^2$, resp., and a high lap-shear strength of (17 ± 4) MPa. Testing at both 140 °C and 200 °C curing temperatures showed that modules with low-filled and highly-filled ECAs achieved comparable initial efficiencies. After damp heat (DH500) testing, modules with capillary suspension ECA showed an efficiency loss of −0.8 % ± 0.4 %, compared to −2.5 % ± 1.1 % for highly-filled ECA. After thermal cycling (TC200), losses were −0.6 % ± 0.5 % versus −1.1 % ± 0.5 %. Both ECA types maintained efficiency losses below 1 % in mechanical load tests. These results demonstrate the potential for silver reduction in shingled solar cell modules through the capillary suspension concept.

## 1. Introduction

First patented in 1956 as conductive cement by Wolfson and Elliott [1] Electrically Conductive Adhesives (ECAs) are now established bonding materials in flip chip, surface mount, advanced packaging and printed circuit board applications [2,3]. In recent years, the solar industry has gained interest in ECAs as cell interconnection material as well [4–7]. In certain applications, Electrically Conductive Adhesives replace the traditional solder bond. Their main advantage is a lower processing temperature of 110–150 °C compared to soldering, which requires temperatures above 200 °C [7]. Additionally, the lead-free adhesives meet the requirements of the RoHS DIR 2011/65/EU directive, which demands lead-free solder [8,9]. Drawbacks of ECAs compared to solder are the need of silver, bleeding, longer processing time and the need of storage at −20 to −40 °C [10]. Concerns regarding lower electrical and thermal conductivity are currently under investigation [11].

Around 95 % of the solar modules produced are connected by tab interconnection [12]. Here, ribbons are used to interconnect the solar cells. The solder bonds joining the ribbon to the cell can be replaced by ECAs without alteration of the module concept [13]. Shingle interconnection is an alternative method to the established tab interconnection of solar cells. In shingle interconnections, solar cells are interconnected by overlapping each other. This allows omitting the ribbons, leading to less shading losses. The principle of shingling is visualised in Fig. 1. This technique allows for particularly high shading resilience [14], reduced ohmic losses [15], a high packing density within the module [16,17] and the realization of visually appealing module designs [18].

This article is part of a special issue entitled: MIW2024 proceedings published in Solar Energy Materials and Solar Cells.

* Corresponding author.
*E-mail address:* marianne.kronsbein@kit.edu (M. Kronsbein).

[1] The first three authors contributed equally.

https://doi.org/10.1016/j.solmat.2025.113603
Received 30 January 2025; Received in revised form 14 March 2025; Accepted 23 March 2025
Available online 26 March 2025

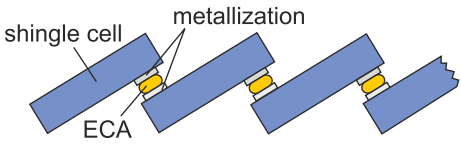


**Fig. 1.** Principle of shingling solar cells. The cells are overlapped and aligned at their busbar metallization, with mechanical and electrical interconnection achieved using an ECA [18].

Temperature cycles during module operation lead to thermo-mechanical stresses within the solar module. In conventional tab interconnection, these stresses can be mitigated by the displacement of solar cells within the intercell gaps. In shingle interconnection, thermo-mechanical stresses can only be alleviated at the bonding joint. For this purpose, the interconnection element must be elastically deformable. Due to its higher flexibility, adhesive bonding using ECAs is significantly better suited for shingle interconnection than solder connections [5,19,20].

ECAs consist of a reactive polymer resin and conductive filler, typically silver. The increasing expansion of photovoltaic (PV) manufacturing capacities results in a rising demand for silver [12]. Without optimizing the specific silver consumption, the existing silver reserves could be largely depleted by 2050 [21]. For this reason, there are ongoing efforts to reduce the silver demand in PV manufacturing. In ECAs, decreasing the percolation threshold by conductivity enhancement through surface treatment of the silver particles [22–24] or by generation of silver nanoparticles [25] is most common to reduce silver consumption.

The percolation threshold, i.e. the filler content at which a material becomes conductive strongly depends on the shape [26] but even more on the colloidal interactions among the particles. It has been shown, that the capillary suspension phenomenon [27,28] is a powerful tool to reduce the percolation threshold and hence enhance the thermal [29,30] or electrical conductivity in composite materials comprising a polymer matrix and dispersed conductive filler particles [31]. Capillary suspensions (CapS) are ternary solid-liquid-liquid systems in which a second immiscible liquid induces the self-assembly of particles into a percolating network structure [27,28]. The particle network strength is controlled by strong capillary forces acting among the particles due to the added secondary liquid. Thus, the composite material typically exhibits a high yield stress, pronounced shear thinning, and fast structural recovery after strong shear [32]. This results in a high stability against sedimentation and phase separation, but makes it also ideally suited for screen printing or dispensing applications [33]. In this way, composite materials with a high electrical conductivity can be generated at a significantly reduced silver consumption.

In this study, we apply the capillary suspension concept on ECAs and compare them to regular ECAs at different silver filler fractions. For evaluation, we give upper and/or lower limits for rheological, electrical and mechanical parameters for uncured and cured ECA based on literature research and own experience. Finally, this work compares modules build with a low-filled and a high-filled ECA regarding their long-term stability against damp heat, thermal cycling and mechanical load.

## 2. Material and methods

### 2.1. Material

In this work, epoxy resin and silver flakes (s. Fig. 2, $x_{50,3}$ app. 11 µm) were used as polymer matrix and conductive filler, resp. The filler volume fraction was varied between 5 and 30 % (which accounts for 33 to 80 weight-%). For one series of experiments only epoxy and silver filler were used, referred to as “regular”. A second series consists of epoxy and silver and an additional secondary liquid, here referred to as “CapS”.

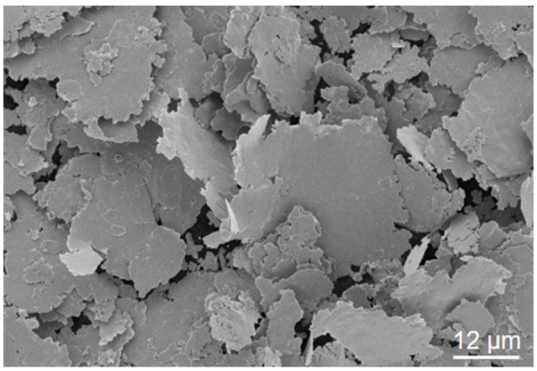


**Fig. 2.** Scanning electron microscopy (SEM) image of silver flakes used in this study.

### 2.2. Differential Scanning Calorimetry

Differential Scanning Calorimetry (DSC) was conducted using a DSC Q200 (TA Instruments) to determine peak curing temperature and curing energy of the samples. Samples where heated at a constant rate of 10 K/min from 40 to 210 °C. Curing energy was calculated in the interval from 70 to 200 °C. Deviations of ±1 K for peak curing temperature and ±3 $\%_{rel}$ for curing energy were found for different measurements of one sample.

### 2.3. Rheological characterization

A rotational rheometer (MARS, Haake) with plate-plate geometry was used for yield stress determination. The shear stress was stepwise increased from 0.1 to 1000 Pa in 81 logarithmic steps and deformation was measured. The yield stress was determined from the intersect of the tangents to the elastic and flow region in a double-logarithmic stress-strain diagram [34]. Formulations were measured three times, each. Average and standard deviation were calculated.

### 2.4. Electrical characterization

For determination of volume resistivity three ECA lines of 4 mm width and 0.1 mm thickness were applied by a squeegee through a stencil on a glass slide. They were cured for 2 min at 150 °C on a heat plate. Three measurements per line were taken via four-point-measurement with a 2450 SourceMeter (Keithley) at a current of 100 mA. Contact resistivity was measured similar to Ref. [35]. Ten silver fingers on a circuit board were connected with an ECA line and cured for 2 min at 150 °C. The contact resistance $\rho_C$ was calculated from 28 measurements of joint resistance $R_J$, ECA bulk resistance $R_B$ and finger resistance $R_F$ according to Eq. (1) with contact area $A$. Average and standard deviation of volume and contact resistivity were calculated.

$$\rho_c = (R_J - R_B - R_F) / 2 \bullet A \qquad \text{Eq. 1}$$

For volume resistivity measurements during curing the set-up from contact resistivity measurement was taken. Four neighbouring silver fingers were connected with the source meter. The circuit board was placed on the heat plate and resistivity was measured over 15 min at 100, 120, 140, 150 and 200 °C, res. via 4-point-measurement.

Long-term storage tests at elevated temperature were conducted with samples containing 10 vol% silver. One regular and one CapS sample was kept for 36 days at 85 °C. Volume and contact resistivity were measured initially and after 18 and 36 days, resp. As reference two samples were stored at room temperature.

### 2.5. Mechanical characterization

Lap-shear strength was determined with a TA.XT plus Texture Analyser (Stable Micro Systems) according to ASTM D1002-10 [36]. Two carbon steel bands were bonded with a joint area of app. 15 $mm^2$. Samples were cured for 10 min at 150 °C in an oven. Tensile stress was applied to the samples at a speed of 0.2 mm/s. Long-term shear tests samples were prepared by bonding two glass slides with an ECA line of 15 mm length, 0.5 mm width and 0.09 mm thickness. Shear stress was applied up to a deformation of 0.1 mm with a speed of 0.1 mm/s based on [37] and released again. 3600 cycles were conducted. The minimum shear stress amplitude during these cycles was taken for determination of long-term reliability. Three samples per ECA were prepared and measured.

### 2.6. Module building and testing

For module testing, Passivated Emitter and Rear Cell (PERC) host cells in G1 format, produced through a mass production process, were utilized. The shingle cells were separated using a laser scribe and mechanical cleaving (LSMC) process. Only the outer shingles in pseudo-square (PSQ) format, with dimensions of 158.75 × 31.75 $mm^2$, were used. Test modules comprising six shingle cells were used for Thermal Cycling (TC) and Damp Heat (DH) tests according to IEC 61215-2. TC testing was conducted without current load. For Mechanical Load (ML) tests, full sized modules were built with ten strings of 32 shingles each. Test conditions followed IEC 61215-2: TC between −40 °C and +85 °C, DH at 85 °C/85 % relative humidity, and ML with static loads of +5400 Pa and −3600 Pa.

To interconnect the cells, a commercially available capillary suspension ECA with filler content between 5 vol% and 10 vol% and a regular suspension ECA with 20 vol% filler particles and the same polymer matrix were used as a reference. The filler content of the regular suspension was adjusted to match the volume resistivity of the capillary suspension ECA, which was measured at (2.9 ± 0.3) $10^{-3}$ Ω cm, as confirmed by four-point measurements. To investigate the influence of perovskite-compatible low-temperature processes on long-term stability, a variation of the curing temperature was conducted. A lower temperature of 140 °C was chosen as it is compatible with perovskite materials [38]. The upper temperature of 200 °C was chosen, as it is a commonly used temperature for interconnecting PERC and heterojunction (HJT) solar cells. This was performed on the modules for TC and DH tests. Full size modules for ML tests were cured at 140 °C.

To interconnect the cells, an prototype shingle stringer from M10 Industries was employed [18]. The ECA was applied using a jet dispensing process. The application of ECA was controlled by adjusting the preheating temperature and the pressure of the dispenser setup. An infrared lamp setup was utilized to cure the ECA. To set the process temperature, the maximum curing temperature was monitored using liquid crystal thermometers affixed to the non-IR-exposed side of the shingle cells. The lamp power was adjusted accordingly.

The modules were laminated in a glass-backsheet configuration using an industrial laminator from Bürkle, model Ypsator M-LAPV 1222-HKV. The peak temperature of the lamination process was 155 °C. The configuration for the produced full-size modules is illustrated in Fig. 3. Mini modules were also produced using the same configuration; however, unlike the full-size modules, the mini modules were not framed.

After module production, the width of the ECA in the shingle joint was measured using an 2D X-ray inspection system (Dage XD7600NT).

Ageing tests were conducted in accordance with IEC 61215-2 MQT 11 (thermal cycling) and MQT 13 (damp heat). One module with low-filled capillary suspension ECA, cured at 140 °C, was set aside as a reference and was not subjected to ageing tests. The reference module is compared to the aged modules to provide an estimation of calendric ageing and measurement uncertainty. To compare the interconnection quality and resilience against ageing, illuminated *IV* curves were recorded to determine module efficiency. Dark *IV* curves were also measured to assess the pseudo series resistance $R_{s*}$, which serves as a representation of interconnection quality. This parameter is less affected by current mismatch due to e.g. inconsistent overlap or different shingle efficiencies than the fill factor *FF* [40]. The value of $R_{s*}$ was extracted through linear interpolation of the dark *IV* curve within the current range of ($-1.9 > I > -2.1$) A.

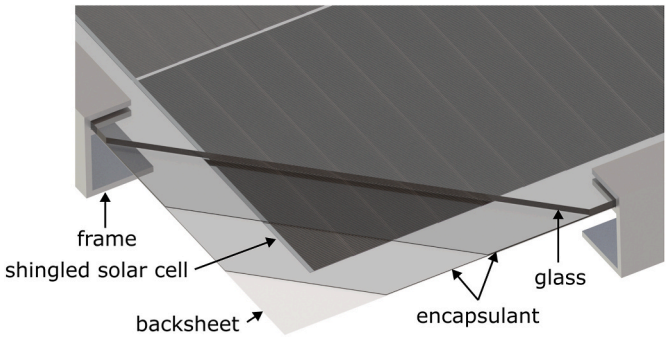


**Fig. 3.** 3D model, illustrating the module setup of the produced full-size modules [39].

## 3. Theory

### 3.1. Capillary suspensions

Composite materials consisting of a polymer and a conductive filler follow a typical behaviour. At a low filler content, the conductivity of the composite is close to that of the polymer. If a certain filler content, the so-called percolation threshold, is reached, small changes in volume fraction of the filler cause an increase in conductivity over several decades. At higher particle volume fractions, the conductivity approaches that of the filler particles [41].

ECAs are mainly formulated as a mixture of a reactive resin and conductive filler particles, but may also include organic solvents or other additives to adjust processing and application properties. Filler particles typically are coated with an appropriate compatibilizer. This promotes deagglomeration of the particles during mixing into the matrix as well as long-term stability against recurring thermo-mechanical stresses, but counteracts the formation of conductive pathways. Therefore, state of the art ECAs typically contain 20 vol% filler or more, way beyond the percolation threshold [42,43].

In capillary suspensions [27,28] the conductive particle network is induced by adding small amounts (typically <1 vol%) of a second liquid, not miscible with the main liquid phase. Capillary suspensions exist either in the pendular state, when the secondary liquid preferentially wets the particles or in the so-called capillary state, when the main fluid preferentially wets the particles. In the pendular state, the secondary liquid forms capillary bridges between the particles. In the capillary state, the particles cluster around secondary liquid droplets, shielding the secondary liquid from the main phase [27,28]. In both cases, sample spanning particle networks self-assemble and may reduce the percolation threshold drastically [29,31]. In ECAs capillary suspensions in the capillary state are favourable as the particles must be compatible with the main phase. A typical characteristic of a capillary suspension is the introduction or significant increase of an existing yield stress in the paste. The particle network strength depends on the interfacial tension, the three-phase contact angle and the coordination number, i.e. the number of liquid bridges. Thus, the yield stress of these systems can be controlled in a wide range by the amount and type of the secondary liquid [27,28]. Due to the, compared to other attractive forces like Van der Waals forces, high capillary forces, the particle network remains stable during drying and curing processes [44,45]. The rupture of the bridges under shear leads to a strong shear thinning behaviour and due

to its relatively small volume fraction, the second liquid barely affects the high shear viscosity. The high yield stress, shear thinning behaviour and a fast structural recovery after cessation of flow are advantageous for the intended screen printing or dispensing application [46,47]. In addition, sedimentation and phase separation, which is a challenge in conductive ECAs due to the high density difference between matrix and filler particles, is prevented because the particles are trapped in the strong network structure, which is beneficial for extended shelf life. Beyond that, additives for particle surface treatment can be directly added to the secondary liquid. These additives are then deposited with the secondary fluid in the contact area between the particles. In ECAs, this can be utilized to remove or replace the compatibilizer at the contact points of the particles only. This results in high conductivity while maintaining the good compatibility between particles and polymer matrix.

Fig. 4 shows schematically the two formulation types investigated in this study. The regular ECA consist of a polymer matrix (green) and silver flakes (grey). The flakes are coated with fatty acids (blue) as compatibilizers, which leads to homogenous distribution of the particles in the polymer matrix. By adding a secondary liquid (orange) a capillary suspension is formed. The secondary liquid is chosen to exhibit a three-phase contact angle beyond 90°, meaning the polymer preferentially wets the particles. This leads to an inhomogeneous particle distribution in form of a (three-dimensional) particle network in the capillary state. The formulation is stabilized and exhibits continuous conductive pathways at low filler content.

### 3.2. Requirements for ECAs in shingled solar cell interconnections

ECAs were initially developed for the electronics industry where they replace the traditional solder bond [1]. Therefore, ECAs are mainly compared with solder and its properties where they often lag behind in conductivity and mechanical reliability [48]. For the application in solar cell interconnection especially in the shingling concept ECAs are valued for their elastic properties [5,35]. Requirements regarding the application process, electrical resistivity or shear strength are still under research [11,20,37]. Thus, solder is often taken as the benchmark. We herein give an overview from own experiments and literature review on requirements regarding the properties of electrically conductive adhesives for application in solar cell shingling.

High-filled ECAs exhibit a stable paste like texture. At low filler content suspensions are prone to sedimentation. For the ECA system given in this paper the introduction of a yield stress greater than 1 Pa was sufficient to prevent sedimentation. According to the well-known Stokes-equation increasing the bulk viscosity would be another means to decrease sedimentation speed, but this would simultaneously affect the application behaviour. Depending on the application process, typically dispensing or screen printing [3], rheological properties must be further adjusted. Whereas dispensing requires primarily a homogeneous, air-free and stable paste, screen printing has more specific requirements regarding shear thinning behaviour, thixotropy or yield stress [46]. In both cases a controlled flow must be guaranteed. In own experiments, it was found that a yield stress between 10 and 100 Pa yields good results for ECAs.

Lower processing temperatures are one of the main advantages of ECAs. Soldering is typically performed above 200 °C. ECAs can already cure below 140 °C, which is required for temperature sensitive solar cells such as perovskite and tandem cells [49,50]. But the low curing temperature comes often with long curing times. To be competitive to the through-put of soldered module production lines a curing time of maximum 30 s is recommended [51]. Therefore, snap-curing resins are of high interest for ECAs. Post-curing during lamination is also an option to reduce initial curing time [52]. ECAs would need to exhibit sufficient mechanical strength for handling and transportation after the first curing step and could be fully cured during lamination. But as electrical conductivity develops during curing [53] electrical performance tests on string level might not be possible.

The volume resistivity of eutectic solder is app. $2 \times 10^{-5}$ Ω cm [3]. Geipel et al. [11] showed that for ribbon-based interconnections an ECA with a volume resistivity of $1 \times 10^{-3}$ Ω cm did not change the fill factor compared to an ECA with $1 \times 10^{-4}$ Ω cm. Fig. 5 shows the absolute efficiency loss of a full-format shingled module with continuous ECA lines depending on the contact and volume resistivity calculated according to Ref. [17]. The power output of the module is 310 W. In the given range of volume resistivity of $10^{-4}$ to $10^{-2}$ Ω cm the contact

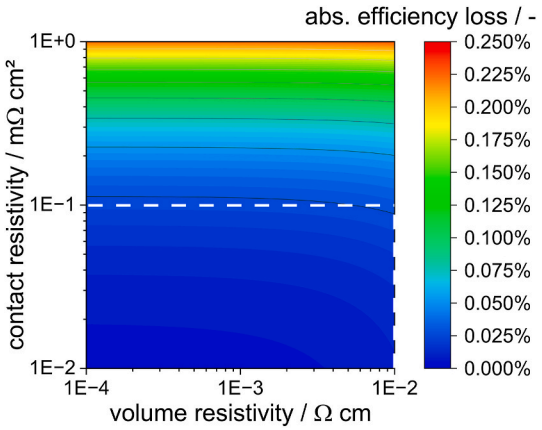


**Fig. 5.** Efficiency loss calculated based on [17] of a full format shingled module bonded with continuous ECA lines of 50 µm thickness and 47.3 mm² area in dependence of volume and contact resistivity, module power is 310 W, current is 8.76 A.

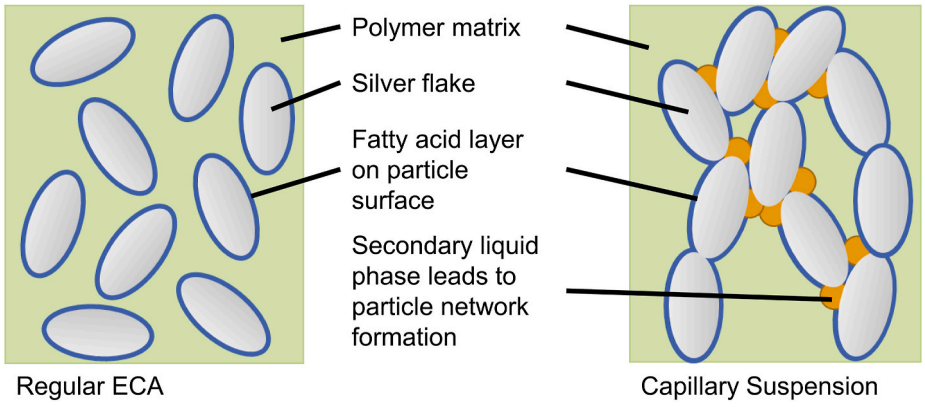


**Fig. 4.** Schematic drawing of the regular and capillary suspension type ECA investigated in this study.

resistivity dominates the efficiency loss. It was found that the influence on the efficiency was negligible when contact resistivity is below $1 \times 10^{-1}$ mΩ cm$^2$ [54]. Thus, a volume resistivity up to $1 \times 10^{-2}$ Ω cm is sufficient with minor impact on module efficiency. An ECA with volume resistivity of $1 \times 10^{-2}$ Ω cm and contact resistivity of $1 \times 10^{-1}$ mΩ cm$^2$ accounts for an absolute efficiency loss of 0.028 % in the considered module.

In shingled modules thermomechanical stress must be compensated within the bond. Beaucarne [20] calculated that the ratio between shear modulus and shear strength should be as low as possible to withstand thermally induced stresses. Therefore, a low shear modulus (<500 MPa) and high shear strength (>10 MPa) is recommended. Additionally, experiments have already shown that mechanical properties play a minor role in module performance as long as the bond does not fail [37,55].

In addition to thermomechanical stresses, shingle solar joints are subjected to various loads during operation, including static loads (e.g., snow, hail) and penetrating moisture. IEC 61215-2 outlines methods for assessing the long-term durability of solar modules. Thermal cycling tests (MQT 11), damp heat tests (MQT 13), and static mechanical load tests (MQT 16) are particularly relevant for shingle interconnections. A test is considered failed if the performance loss of the tested solar module is at least 5 %.

## 4. Results and discussion

Regular ECAs based on epoxy resin and silver flakes were prepared with different filler content to determine the percolation threshold for paste stability and electrical conductivity. A capillary suspension based ECAs is shown to decrease both thresholds. The influence of the particle volume fraction as well as the secondary liquid contained in the capillary suspension based ECA on the ECA's properties in the uncured and cured state as well as during curing were investigated. A highly-filled regular ECA is compared to a low-filled capillary suspension based ECA as interconnection material in solar modules.

### 4.1. Uncured ECA

The yield stress was determined as an indicator of the paste's stability against sedimentation and phase separation. Low-filled ECAs formulated as a regular suspension do not exhibit a yield stress. As shown in Fig. 6, only pastes with a filler volume fraction of 15 vol% and above possess a yield stress. The sample with 15 vol% silver flakes has a yield stress of (3 ± 1) Pa. The yield stress increases exponentially with increasing filler amount to (136 ± 27) Pa at 30 vol% filler content. In the given regular ECA, at least 15 vol% silver flakes are necessary to fulfil requirements regarding application by dispensing. To reduce silver content a stabilization mechanism is necessary. The ECA based on the capillary suspension concept possesses a yield stress even at a low filler volume fraction of 5 % with (5 ± 3) Pa. This is due to strong attractive interactions induced by the secondary liquid. At higher volume fractions of 10–20 %, the yield stress increases to (63 ± 3) Pa, essentially independent of filler content. For the ECA investigated here, a silver content as low as 5 vol% is sufficient to provide sedimentation stability and suitability for dispensing when the capillary suspension concept is applied. Visual inspection did not reveal indications of phase separation even after twelve days of storage at 22 and 8 °C, resp. For screen printing, a yield stress above 10 Pa is required and therefore, higher particle volume fractions are mandatory. A particle volume fraction between 5 and 10 vol% in capillary suspension based ECAs is necessary compared to standard ECAs where at least 20 vol% silver is required to guarantee screen printability.

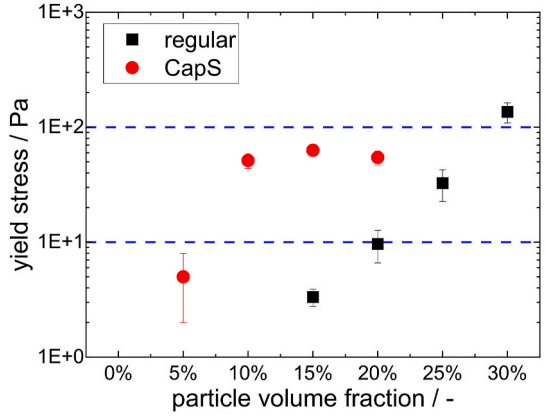


**Fig. 6.** Yield stress of uncured ECAs with 5–30 vol% Ag for regular ECAs (black squares) and 5 to 20 vol% Ag for capillary suspension concept ECAs (red circles), regular ECAs with 5 and 10 vol% do not exhibit a yield stress, the dotted lines indicate limits of recommended yield stress. (For interpretation of the references to colour in this figure legend, the reader is referred to the Web version of this article.)

### 4.2. Curing

DSC measurements were carried out to determine whether the secondary liquid in the capillary suspension-based ECA affected the curing reaction. Fig. 7a shows the heat flow of ECA samples with 10 vol% silver without and with secondary phase as a function of temperature. Temperature was increased by 10 K per minute. Results are shown for 50–205 °C. For a regular ECA, curing initiates at 84 °C and heat flow reaches a peak at 101.7 °C with 2.1 W/g, then up to 108 °C the heat flow decreases symmetrically. At higher temperatures, the decrease in heat flow is lower. Curing occurs up to 200 °C with steadily decreasing heat flow. For the ECA with the secondary liquid phase, the curing reaction starts at 97 °C which is 15 K higher than for the regular ECA. The increase of the heat flow, however, is steeper and reaches a maximum at 108.8 °C and 3.2 W/g, it then deceases symmetrically up to 118 °C where the curve falls onto the curve of the regular ECA. As expected, the total curing energy was the same for both ECAs with 273.1 and 273.7 J/g, resp. The utilized secondary liquid retards the initiation of curing but was selected not to be part of the curing reaction.

Fig. 7b shows the peak curing temperature and curing energy per weight of regular ECAs in dependence of the filler volume fraction determined by DSC. The peak curing temperature increases slightly from 94 °C for the pure resin to 111 °C for an ECA filled with 30 vol% particles. This is presumably due to the higher thermal conductivity of the particles compared to the resin. The thermal energy input will preferably lead to a temperature increase of the particles and then to curing of the resin. The peak curing temperature of ECAs containing a secondary phase is generally 7–9 K higher than the corresponding ECA without secondary phase. All tested ECAs cure at a temperature below 140 °C which is often required for low temperature applications. The curing energy per weight decreases from 535.2 J/g of the pure epoxy by 31, 49, 61, 68, 75 and 79 %, resp. with increasing particle volume fraction to 110.8 J/g at 30 vol% Ag. This corresponds well with the weight fraction of particles which account for 33, 51, 62, 70, 76 and 80 wt%, resp. This indicates that the particles have only minor influence on the curing reaction. The difference might be due to the compatibilizers on the particle surface or the value for the pure epoxy was underestimated.

The PV industry requires an ECA with low curing temperature and fast curing to guarantee high throughput. Low-temperature curing was confirmed by DSC. The required curing time mainly depends on the evolution of conductivity during curing. A capillary suspension concept based ECA with 10 vol% silver was cured at 100, 110, 120, 140, 150 and 200 °C, respectively. The volume resistivity was monitored over 15 min. Fig. 8 shows the resistivity curves for this ECA over curing time. With the first touch on the heat plate, the volume resistivity decreases to $2 \times 10^{-2}$ Ω cm regardless of the temperature. Within 50 s the volume resistivity decreases by at least one order of magnitude irrespective of the curing

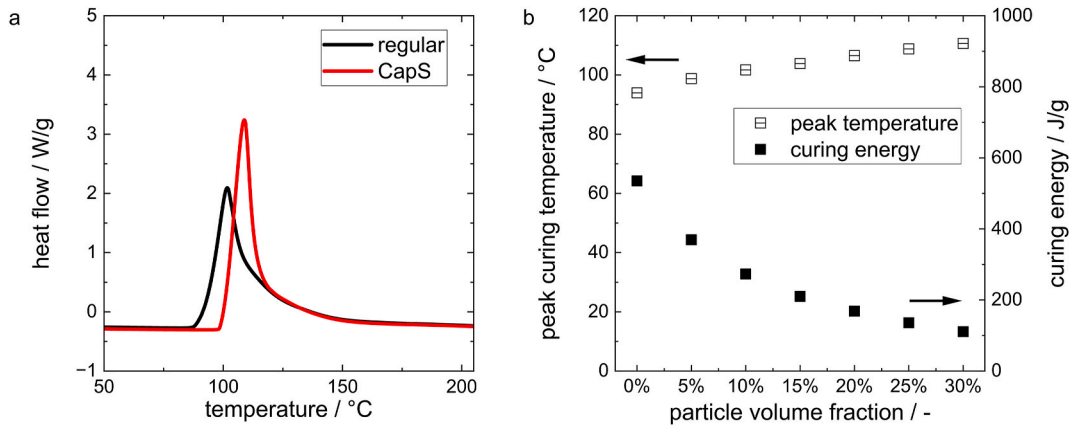


**Fig. 7.** a) DSC curves of a regular ECA (black) and a capillary suspension based ECA (red), both samples contain 10 vol% Ag, b) Peak curing temperature (open squares) and curing energy per weight (filled squares) for regular ECAs with filler content between 0 and 30 vol%. (For interpretation of the references to colour in this figure legend, the reader is referred to the Web version of this article.)

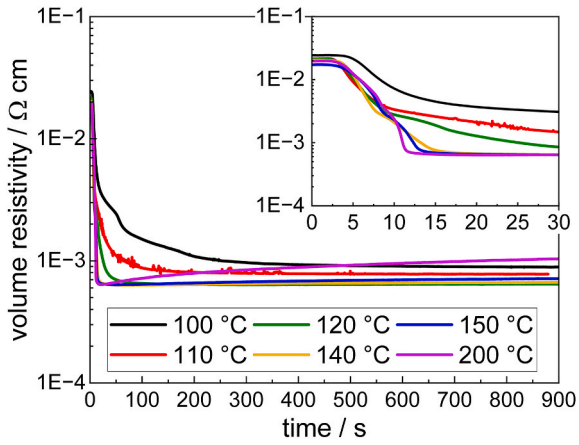


**Fig. 8.** Development of volume resistivity over curing time of a capillary suspension based ECA with 10 vol% Ag filler at curing temperatures of 100, 110, 120, 140, 150 and 200 °C, resp. over 15 min, Inset: over the first 30 s.

temperature. The sample cured at 100 °C reaches a volume resistivity of $9.3 \times 10^{-4}$ Ω cm after 400 s which only decreases slightly to $8.9 \times 10^{-4}$ Ω cm after 15 min curing time. A curing temperature of 110 °C leads to an approximately constant resistivity value of $7.8 \times 10^{-4}$ Ω cm after 160 s. With both curing temperatures, 100 and 110 °C, the minimum volume resistivity of $6.4 \times 10^{-4}$ Ω cm measured at higher curing temperatures cannot be reached within 15 min. This indicates an incomplete curing of the sample and is in line with DSC measurements. At curing temperatures of 120, 140, 150 and 200 °C, res. the samples exhibit the minimum value of $6.4 \times 10^{-4}$ Ω cm after 140, 30, 26 and 16 s, respectively (Fig. 8 inset). We assign the irregular trend between 5 and 10 s to the heat transfer through the circuit board. Therefore, a curing temperature of at least 140 °C is required for the investigated materials to be competitive to soldering when it comes to manufacturing speed. When curing time does not matter a curing temperature of 120 °C is sufficient for full curing. Curing speed will differ on different substrates and with different heat sources.

The results indicate as well that samples should not be kept too long at elevated temperatures above 150 °C. After app. 110 s at 150 °C and 30 s at 200 °C an "over-curing" effect occurs where the volume resistivity increases again. The effect is more pronounced at the higher curing temperature of 200 °C and leads to an increase in resistivity to $10.0 \times 10^{-4}$ Ω cm after 15 min curing. As cell strings are exposed to elevated temperature during the lamination step an experiment was conducted where an ECA with 10 vol% silver and secondary phase was cured at 150 °C with different curing times. Afterwards, samples were left to cool down to room temperature and then kept on a heat plate for another 10 min at 150 °C. The results of volume resistivity measurements are shown in Table 1. As expected, the volume resistivity is lower after short curing times with approximately $7.0 \times 10^{-4}$ Ω cm after 60–90 s of curing and increases for increasing curing times. When samples are exposed for another 10 min to 150 °C the volume resistivity only alters within the experimental uncertainty. Therefore, the over-curing effect does not occur once the samples have cooled down.

### 4.3. Cured ECA

Once cured, ECAs guarantee the electrical and mechanical interconnection in shingled solar modules. Both properties highly depend on the filler volume fraction. Whereas low resistivity is favoured at higher filler content, good mechanical properties require low fill grades. We show that ECAs based on the capillary suspension concept combine low resistivity and low filler content. Furthermore, the long-term stability is investigated.

#### 4.3.1. Electrical properties

For determination of the volume and contact resistivity samples were cured for 2 min at 150 °C. Fig. 9a shows the results of the volume resistivity in dependence of the particle volume fraction of ECAs with and without secondary liquid phase. Regular ECAs with 5 and 10 vol%, respectively, exhibit high volume resistivities of 59 and 18 Ω cm. The standard deviation is high as the ECAs exhibit insulating and conductive areas at this low degree of filling. When the silver fraction is increased to 15 vol%, the percolation threshold for electrical conductivity is passed and the volume resistivity drops to $(11.6 \pm 3.1)\ 10^{-3}$ Ω cm. With further increase of particle volume fraction the volume resistivity further decreases to $(1.1 \pm 0.1)\ 10^{-3}$ Ω cm at 30 vol%. The capillary suspension concept reduces the percolation threshold for electrical conductivity

**Table 1**
Volume resistivity of a capillary suspension based ECA with 10 vol% Ag filler before and after post-curing at 150 °C for 10 min in dependence of initial curing time at 150 °C.

| Curing time (150 °C) | Before post-curing $10^{-4}$ Ω cm | After post-curing (150 °C, 10 min) $10^{-4}$ Ω cm |
|---|---|---|
| 30 s | (6.3 ± 0.2) | (6.1 ± 0.3) |
| 60 s | (7.0 ± 0.6) | (6.8 ± 0.4) |
| 90 s | (6.9 ± 0.3) | (6.8 ± 0.3) |
| 120 s | (7.9 ± 0.9) | (7.7 ± 1.1) |
| 5 min | (8.2 ± 0.2) | (8.4 ± 0.3) |
| 10 min | (9.1 ± 0.7) | (8.6 ± 0.3) |

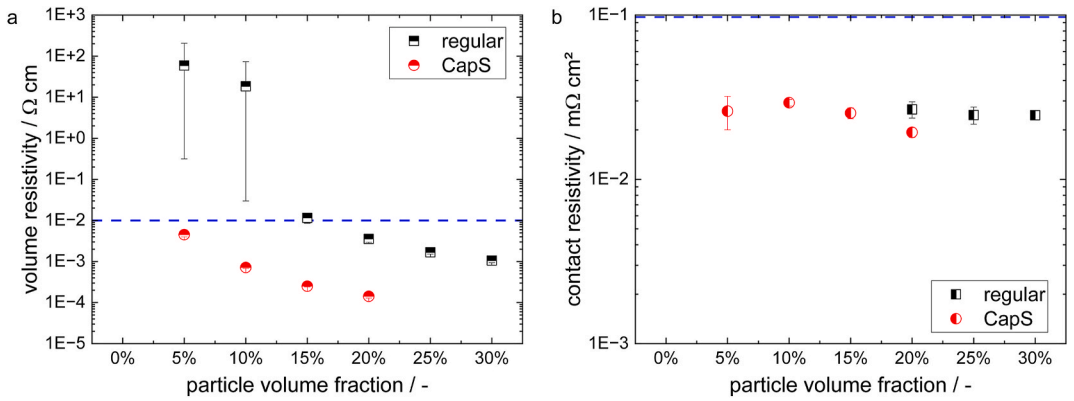


**Fig. 9.** a) Volume resistivity and b) contact resistivity against silver of regular ECAs (black squares) with filler fractions of 5–30 vol% and capillary suspension concept ECAs (red circles) with 5–20 vol% silver filler, contact resistivities of regular ECAs with 5–15 vol% Ag were not measurable, dotted lines represent the upper limit of resistivity. (For interpretation of the references to colour in this figure legend, the reader is referred to the Web version of this article.)

below 5 vol%. The secondary liquid distributes between the particles and induces a network structure, wherein the particles come in contact and form conductive pathways. An ECA with secondary liquid phase exhibits a volume resistivity of (4.5 ± 0.5) $10^{-3}$ Ω cm at 5 vol% silver already, which is lower than that of a regular ECA with three times higher filler content. Above the percolation threshold, the capillary suspension based ECAs investigated here have a one order of magnitude lower resistivity compared to the regular ECAs. The resistivity decreases with increasing particle volume fraction to (0.14 ± 0.01) $10^{-3}$ Ω cm at 20 vol% silver. Solar cell interconnection by shingling requires a volume resistivity below 1 × $10^{-2}$ Ω cm (when low contact resistivity is given). Whereas in regular ECAs more than 15 vol% are necessary to fulfil this requirement, the silver amount can be significantly reduced to 5 vol% silver by addition of a secondary liquid phase.

Contact resistivity against silver was determined for the same ECAs. Results are shown in Fig. 9b. When the volume resistivity is higher than 1 × $10^{-2}$ Ω cm contact resistivity cannot be calculated as the deviation in volume resistivity becomes the same order of magnitude as the contact resistivity. Therefore, only results for regular ECAs filled with 20 vol % silver and above are shown. The contact resistivity varies in a narrow range between 0.02 and 0.03 mΩ $cm^2$ for all formulations, regardless of the presence of a secondary liquid phase and volume fraction. This is counter intuitive as one might expect decreasing contact resistivity with increasing filler content. We believe that the silver flakes align parallel to the contact area due to the application using a squeegee. Therefore, very good contact between particles and metallization fingers is always given irrespective of filler volume fraction and contact resistivity is comparably low. The results confirm contact resistivity values below 0.1 mΩ $cm^2$, which is sufficient for shingling interconnection.

The long-term stability of the electrical properties was monitored for 36 days to determine any effects of the uncured secondary liquid. A sample without and one with secondary liquid phase, resp. and 10 vol% silver fraction were kept at 85 °C. Reference samples were stored at room temperature. Measurements were taken on the initial day, day 18 and day 36. Fig. 10a shows the volume resistivity of these samples. The initial volume resistivities were (18 ± 3) $10^{-3}$ Ω cm and (22 ± 2) $10^{-3}$ Ω cm for the samples without secondary liquid phase and (0.71 ± 0.04) $10^{-3}$ Ω cm and (0.63 ± 0.04) $10^{-3}$ Ω cm for capillary suspension based samples. In regular ECAs post-curing occurs which is more pronounced at elevated temperature. It leads to a resistivity drop to (5.5 ± 0.5) $10^{-3}$ Ω cm at 85 °C and (14 ± 1) $10^{-3}$ Ω cm at room temperature after 18 days. The volume resistivity of ECAs with secondary phase remains constant both at 85 °C and room temperature over 36 days. The same accounts for the contact resistivity (Fig. 10b), which also does not change over storage time and exhibits a value of (0.034 ± 0.003) mΩ $cm^2$ for the capillary suspension based ECA. The secondary liquid does not deteriorate the long-term stability of the ECA. Contact resistivity for the regular ECA could only be determined for the post-cured samples at 85 °C with similar results to the Capillary Suspension based ECA. These results are promising for a module life-time of more than 30 years regarding the electrical performance.

### 4.3.2. *Mechanical properties*

Shingled modules consist of overlapping solar cells which are bonded by an ECA. Therefore, the lap-shear test was performed to characterize the adhesive or cohesive strength of the ECAs. Fig. 11a shows the lap-shear strength of ECAs including between 5 and 30 vol% silver with and without secondary liquid. The lap-shear strength decreases

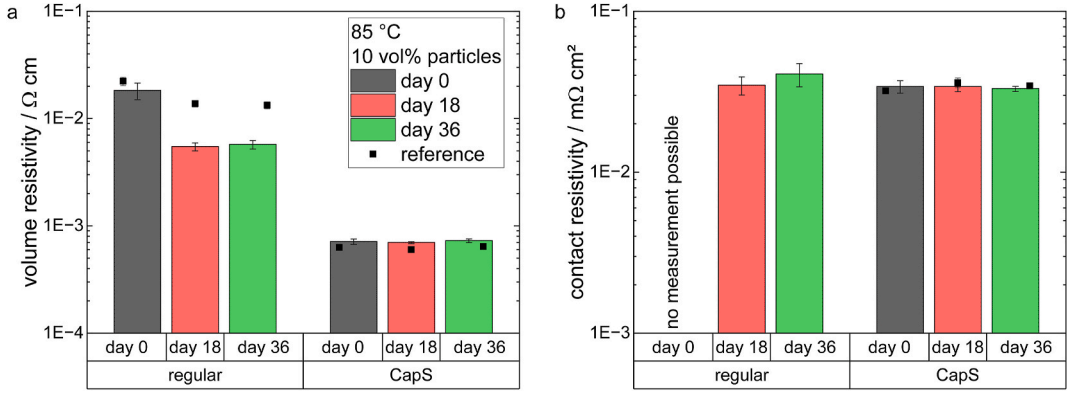


**Fig. 10.** a) Volume resistivity and b) Contact resistivity of regular and capillary suspension based ECAs with 10 vol% particles on day 0, 18 and 36 after storage at 85 °C and room temperature as reference.

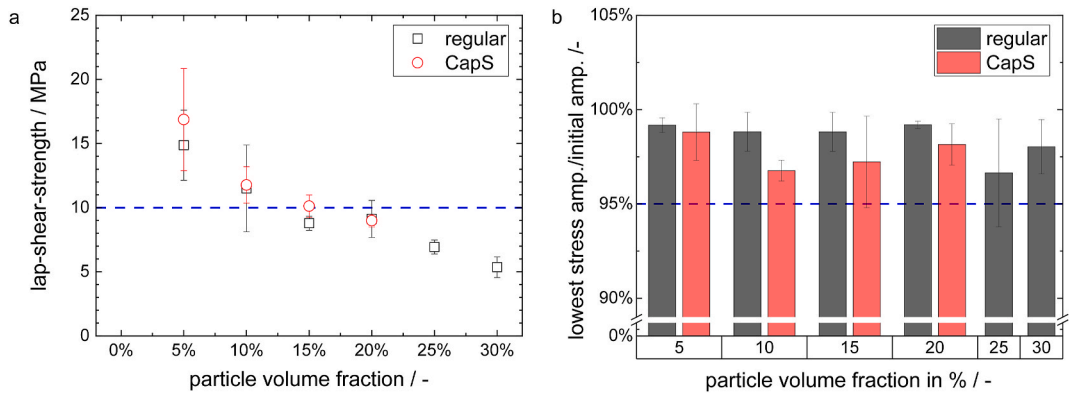


**Fig. 11.** a) Lap-shear strength in dependence of particle volume fraction of regular (black squares) and capillary suspension based (red circles) ECAs, the dotted line indicates the lower limit of recommended lap-shear strength, b) Lowest stress amplitude during 3600 cycles of shear normalized with the initial stress amplitude of regular (black) and capillary suspension based (red) ECAs with filler content between 5 and 30 vol%, the dotted line indicates 95 % of initial strength. (For interpretation of the references to colour in this figure legend, the reader is referred to the Web version of this article.)

approximately linearly with increasing filler volume fraction from (15 ± 2) MPa at 5 vol% to (5 ± 1) MPa at 30 vol%. At 5 vol% filler fraction adhesive and cohesive failure occurs, whereas at higher filler content only cohesive failure is present. As expected, every additional particle weakens the polymer matrix which is responsible for the mechanical strength. A particle network induced by capillary forces does not strengthen the ECA in the cured state. The lap-shear strength of ECAs with secondary liquid phase does not differ from the ones without. The lap-shear strength is independent of the particle distribution and the addition of small amounts of non-curing secondary liquid. For shingling a lap-shear strength of at least 10 MPa is required, and for the polymer matrix given here the filler content should not exceed 15 vol%.

To determine long-term stability under cyclic load two glass slides were bonded with ECA and exposed to 3600 cycles of periodically varying shear with a maximum amplitude of 0.1 mm. Fig. 11b shows the lowest stress amplitude of the sample during 3600 cycles normalized with the initial stress amplitude. All samples retain more than 95 % of the initial strength during 3600 cycles irrespective of filler volume fraction or presence of secondary liquid phase, except for one outlier (out of three samples) at a filler content of 25 vol%. These results indicate a high probability, that modules built with the given ECA can operate 30 years or more without mechanical failure.

### 4.4. Module performance

So far, we have shown that regular ECAs with 20 vol% silver exhibit rheological and electrical properties that have been found suitable for shingling applications. On the other hand, for the epoxy/silver system investigated here less than 15 vol% filler is necessary to get an ECA with acceptable bonding strength. The capillary suspension concept enabled a reduction of silver content to 5 vol%, while maintaining electrical and mechanical properties comparable to highly-filled regular suspension ECAs, though showing different rheological behaviour. For the module tests, a capillary suspension based ECA with filler content between 5 and 10 vol% was selected, referred to as low-filled ECA. The filler content was chosen to match the volume resistivity of a highly-filled (20 vol %/70 wt% silver) regular ECA based on the same raw materials. Properties of the low-filled ECA are listed in Table 2.

**Table 2**
Rheological, electrical and mechanical properties of the low-filled ECA.

| Property | Value |
|---|---|
| Yield Stress | (26 ± 2) Pa |
| Volume Resistivity (150 °C) | (2.9 ± 0.3) $10^{-3}$ Ω cm |
| Contact Resistivity (150 °C) | (0.033 ± 0.003) mΩ $cm^2$ |
| Lap-Shear Strength (150 °C) | (14.2 ± 1.7) MPa |

To assess the impact of curing temperatures at the higher range (200 °C) and a more moderate level (140 °C), which is particularly suitable for temperature-sensitive perovskite solar cells, modules were produced under both conditions. The distinct rheological properties of the two evaluated materials affected the volume of dispensed ECA, leading to differences in the applied material quantity. The width of the ECA in the shingle joint was determined using X-ray microscopy. The width of the jet dispensed ECA lines in modules with highly-filled ECA measured (445 ± 80) µm, while the ECA width in modules with low-filled ECA measured (316 ± 74) µm.

The initial module efficiencies calculated based on aperture area are illustrated in Fig. 12a (represented by fully filled boxes). On average, modules interconnected with the highly-filled ECA exhibited slightly higher efficiencies. However, the differences between the groups were within the range of the standard deviation and, therefore, not statistically significant. The groups with low-filled ECA demonstrate lower standard deviations.

The pseudo series resistances are also shown in Fig. 12a (hatched boxes). Similar to the module efficiency, only minor differences are observed between the groups, indicating that the interconnection quality remains comparable for both ECAs and curing temperatures [40].

The results of the aging tests are presented in Fig. 12b. Notably, the efficiency losses across all groups remain well below the critical threshold of 5 % relative loss, indicating that both tests were successfully passed and suggesting good durability of the materials under the tested conditions. However, after DH testing, the group utilizing highly-filled ECA, cured at 140 °C, exhibits significantly higher efficiency losses compared to the other groups. Given the thermal conductivity of the filler particles, enabling efficient heat distribution during curing, it is unlikely that these losses stem from insufficient curing (see Chapter 4.2). In both TC and DH testing, modules interconnected with low-filled ECA exhibit, within the range of the standard deviation, lower efficiency losses. This effect is attributed to the lower filler fraction, which reduces the shear modulus and line width, thereby leading to a lower elastic section modulus.

To evaluate the mechanical load tests, *IV* characteristics were recorded, and the relative losses of short circuit current $I_{sc}$, open circuit voltage $U_{oc}$, fill factor *FF*, and efficiency $\eta$ were determined. The corresponding results are presented in Fig. 13.

Efficiency losses were primarily attributed to a decreased fill factor and a reduction in short-circuit current. The module manufactured using the regular suspension ECA exhibited a higher efficiency loss, mainly driven by a more pronounced decline in the fill factor. In both modules, the efficiency losses were below 1 %. In a statistical investigation of ML

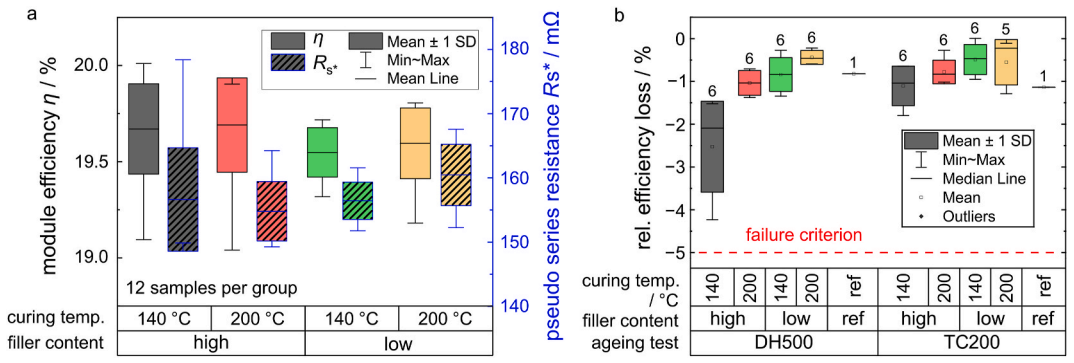


**Fig. 12.** *IV* characteristics of six-cell mini modules. Gray and red bars refer to the regular ECA with 20 vol% silver content, green and yellow bars refer to the capillary suspension based ECA with low silver content. Fully filled boxes denote the efficiency (η), whereas hatched boxes denote the pseudo series resistance $R_{s^*}$. Both ECAs were cured at 140 °C (grey, green) and 200 °C (red, yellow). a) Initial efficiency from illuminated *IV* curves and pseudo series resistance, derived from dark *IV* curves. b) Relative efficiency losses after ageing tests. The group size is shown above the boxes. (For interpretation of the references to colour in this figure legend, the reader is referred to the Web version of this article.)

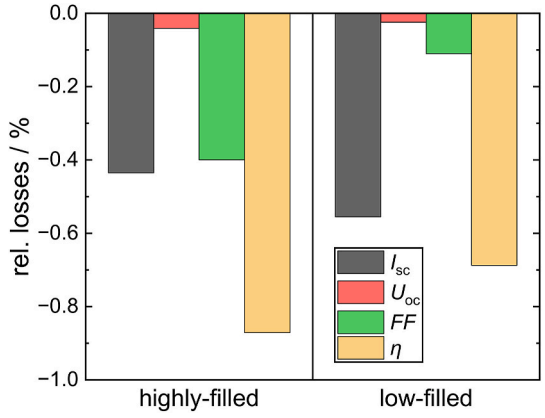


**Fig. 13.** Results of mechanical load tests on two individual solar modules. Relative losses in short circuit current $I_{SC}$ (grey), open circuit voltage $U_{OC}$ (red), fill factor *FF* (green) and efficiency η (yellow) are shown. (For interpretation of the references to colour in this figure legend, the reader is referred to the Web version of this article.)

tests with a maximum load of 5400 Pa from the years 2008–2019, 16.98 % of all modules did not pass the test with a performance loss exceeding 5 %. The average performance loss of all modules in this study was 1.76 % [56]. Compared to these historical data, the shingle modules produced in this study demonstrate an above-average resilience to mechanical loads.

## 5. Conclusion

This work shows the silver saving potential in Electrically Conductive Adhesives and presents a formulation concept for its implementation. The chosen epoxy resin cures fast (<30 s) and at low temperature (<140 °C). The required yield stress between 10 and 100 Pa as well as a volume resistivity below $10^{-2}$ Ω cm and contact resistivity below 0.1 mΩ $cm^2$, once cured, can be achieved by adding 20 vol% of silver flake filler. For a lap-shear strength beyond 10 MPa the filler fraction must be kept below 15 vol% filler. By adding a small amount (<1 vol%) of a secondary immiscible liquid a sample-spanning particle network can be induced even at 5 vol% silver filler. This capillary suspension type formulation is stable and exhibits sufficient volume and contact resistivity of (4.5 ± 0.5) $10^{-3}$ Ω cm and (0.026 ± 0.006) mΩ $cm^2$, resp., as well as superior mechanical strength (lap-shear strength of (17 ± 4) MPa) in the cured state. The secondary liquid does not influence the very good long-term stability of the ECA. By applying the capillary suspension concept a low-filled ECA with good electrical and mechanical properties can be formulated.

The transfer of these material science findings to module level showed promising results: The capillary suspension ECA with a silver content between 5 and 10 vol% achieved the same initial module efficiency and pseudo series resistance as conventional ECAs with 20 vol% filler. Both ECA formulations passed TC200 and DH500 testing in six-shingle mini modules, with the low-filled version cured at 200 °C showing the lowest efficiency losses. In mechanical load tests, efficiency losses remained below 1 %, with the capillary suspension ECA performing comparably well due to its enhanced flexibility resulting from the lower filler content.

In summary, formulating Electrically Conductive Adhesives as capillary suspensions present significant silver saving potential for the photovoltaic industry. Compared to state-of-the-art silver filled ECAs more than 50 % silver can be saved without losses in electrical conductivity or module performance but with gain in mechanical strength.

## CRediT authorship contribution statement

**Marianne Kronsbein:** Writing – review & editing, Writing – original draft, Visualization, Investigation. **Leonhard Böck:** Writing – review & editing, Writing – original draft, Investigation. **Katrin Dyhr:** Writing – review & editing, Writing – original draft, Methodology. **Torsten Rößler:** Writing – review & editing, Supervision. **Norbert Willenbacher:** Writing – review & editing, Supervision, Funding acquisition.

## Funding sources

This work was funded by the German Federal Ministry of Economics and Climate Action (BMWK) as part of the project “Mod30+” with the grant number 03EE1160.

## Declaration of competing interest

The authors declare that they have no known competing financial interests or personal relationships that could have appeared to influence the work reported in this paper.

## Acknowledgements

The authors like to thank Vincent Charlot and Frederic Durand of PROTAVIC INTERNATIONAL Laboratory for their professional support.

## Data availability

The data that has been used is confidential.

## References


[1] H. Wolfson, G. Elliott, Electrically conductive cements containing epoxy resin and silver. https://patentimages.storage.googleapis.com/3f/11/41/116238f66323b0/US2774747.pdf, 1956.

[2] Y. Li, D. Lu, C.P. Wong, Electrical Conductive Adhesives with Nanotechnologies, Springer US, 2010, https://doi.org/10.1007/978-0-387-88783-8.

[3] M.J. Yim, Y. Li, K. Moon, K.W. Paik, C.P. Wong, Review of recent advances in electrically conductive adhesive materials and technologies in electronic packaging, J. Adhes. Sci. Technol. 22 (2008) 1593–1630, https://doi.org/10.1163/156856108X320519.

[4] J.-N. Jaubert, J. Cai, B.X.J. Yu, R. Lv, Y. Lu, T. Xu, G. Zhang, Service lifetime prediction of electrically conductive adhesives-based shingled PV module, IEEE J. Photovoltaics 12 (2022), https://doi.org/10.1109/JPHOTOV.2022.3141343.

[5] L. Theunissen, B. Willems, J. Burke, D. Tonini, M. Galiazzo, A. Henckens, Electrically conductive adhesives as cell interconnection material in shingled module technology, in: 2018 AIP Conference Proceedings, 1999, 2018 080003, https://doi.org/10.1063/1.5049305.

[6] J.J. Jang, J.E. Park, D.S. Kim, W.S. Choi, D. Lim, A comparison analysis on the efficiency of solar cells of shingled structure with various ECA materials, Kses 39 (2019) 1–9, https://doi.org/10.7836/kses.2019.39.4.001.

[7] S. Schwertheim, M. Scherff, T. Mueller, W.R. Fahrner, H.C. Neitzert, Lead-free electrical conductive adhesives for solar cell interconnectors, in: 2008 33rd IEEE Photovolatic Specialists Conference, PVSC 2008. Proceedings, vol. 3, IEEE, 2008, pp. 1–6, https://doi.org/10.1109/PVSC.2008.4922588.

[8] S. Maranghi, M.L. Parisi, R. Basosi, A. Sinicropi, The critical issue of using lead for sustainable massive production of perovskite solar cells: a review of relevant literature, Open Res. Europe 1 (2021) 44, https://doi.org/10.12688/openreseurope.13428.2.

[9] DIRECTIVE 2011/65/EU of the EUROPEAN PARLIAMENT and of the COUNCIL of 8 June 2011 on the Restriction of the Use of Certain Hazardous Substances in Electrical and Electronic Equipment, 2011.

[10] M.I. Devoto, T. Timofte, A. Halm, D. Tune, Measuring the contact resistivity of eca-based joints. https://doi.org/10.4229/EUPVSEC20202020-4AV.1.26, 2020.

[11] T. Geipel, M. Meinert, A. Kraft, U. Eitner, Optimization of electrically conductive adhesive bonds in photovoltaic modules, IEEE J. Photovoltaics 8 (2018) 1074–1081, https://doi.org/10.1109/JPHOTOV.2018.2828829.

[12] VDMA, International Technology Roadmap for Photovoltaics (ITRPV), 2023 Results, fifteenth ed., May 2024, 2024, https://www.vdma.org/international-technology-roadmap-photovoltaic.

[13] K. Hartman, P. Hacke, M. Owen-Bellini, Y. Jin, M. Cummings, A. Taylor, J. Pretorius, L. Fritzemeier, Validation of advanced photovoltaic module materials and processes by combined-accelerated stress testing (C-ast), in: 2019 IEEE 46th Photovoltaic Specialists Conference, PVSC 2019, IEEE, 2019, pp. 2243–2248, https://doi.org/10.1109/PVSC40753.2019.8980545.

[14] N. Klasen, F. Lux, J. Weber, T. Roessler, A. Kraft, A comprehensive study of module layouts for silicon solar cells under partial shading, IEEE J. Photovoltaics 12 (2022) 546–556, https://doi.org/10.1109/JPHOTOV.2022.3144635.

[15] D. Tonini, G. Cellere, M. Bertazzo, A. Fecchio, L. Cerasti, M. Galiazzo, Shingling technology for cell interconnection: technological aspects and process integration, Energy Proc. 150 (2018) 36–43, https://doi.org/10.1016/j.egypro.2018.09.010.

[16] N. Klasen, A. Mondon, A. Kraft, U. Eitner, Shingled cell interconnection: a new generation of bifacial PV-modules, SSRN J. (2018), https://doi.org/10.2139/ssrn.3152478.

[17] M. Mittag, T. Zech, M. Wiese, D. Blasi, M. Ebert, H. Wirth, Cell-to-Module (CTM) analysis for photovoltaic modules with shingled solar cells, in: 2017 IEEE 44th Photovoltaic Specialist Conference (PVSC), IEEE, 2017, pp. 1531–1536, https://doi.org/10.1109/PVSC.2017.8366260.

[18] D. Von Kutzleben, T. Roessler, M. Mittag, J. Weber, S. Sigdel, N. Klasen, P. Zahn, A. Kraft, H. Neuhaus, Development of shingle matrix technology for integrated PV applications, 8th world conference on photovoltaic, Energy Convers. 541–550 (2022), https://doi.org/10.4229/WCPEC-82022-3CO.4.4, 10 pages, 14068 kb.

[19] N. Klasen, Schindelfügestellen in Photovoltaischen Solarmodulen, Karlsruher Institut für Technologie, Dissertation, 2023.

[20] G. Beaucarne, Materials challenge for shingled cells interconnection, Energy Proc. 98 (2016) 115–124, https://doi.org/10.1016/j.egypro.2016.10.087.

[21] B. Hallam, M. Kim, Y. Zhang, L. Wang, A. Lennon, P. Verlinden, P.P. Altermatt, P. R. Dias, The silver learning curve for photovoltaics and projected silver demand for net-zero emissions by 2050, Progr. Photovo. 31 (2023) 598–606, https://doi.org/10.1002/pip.3661.

[22] C. Li, Q. Li, L. Cheng, T. Li, H. Lu, L. Tang, K. Zhang, S. E, J. Zhang, Z. Li, Y. Yao, Conductivity enhancement of polymer composites using high-temperature short-time treated silver fillers, Compos. Appl. Sci. Manuf. 100 (2017) 64–70, https://doi.org/10.1016/j.compositesa.2017.05.007.

[23] Y. Li, K. Moon, C.P. Wong, Electrical property improvement of electrically conductive adhesives through in-situ replacement by short-chain difunctional acids, IEEE Trans. Compon. Packag. Technol. 29 (2006) 173–178, https://doi.org/10.1109/TCAPT.2006.870388.

[24] Q. Fan, H. Cui, C. Fu, D. Li, X. Tang, Z. Yuan, L. Ye, J. Liu, The effect of functionalized silver on rheological and electrical properties of conductive adhesives, ECS Trans. 34 (2011) 811–816, https://doi.org/10.1149/1.3567678.

[25] N. Matsuhisa, D. Inoue, P. Zalar, H. Jin, Y. Matsuba, A. Itoh, T. Yokota, D. Hashizume, T. Someya, Printable elastic conductors by in situ formation of silver nanoparticles from silver flakes, Nat. Mater. 16 (2017) 834–840, https://doi.org/10.1038/nmat4904.

[26] W. Qiao, H. Bao, X. Li, S. Jin, Z. Gu, Research on electrical conductive adhesives filled with mixed filler, Int. J. Adhesion Adhes. 48 (2014) 159–163, https://doi.org/10.1016/j.ijadhadh.2013.07.001.

[27] E. Koos, N. Willenbacher, Capillary forces in suspension rheology, Science 331 (2011) 897–900, https://doi.org/10.1126/science.1199243.

[28] E. Koos, N. Willenbacher, Particle configurations and gelation in capillary suspensions, Soft Matter 8 (2012) 3988–3994, https://doi.org/10.1039/C2SM07347A.

[29] H. Sun, X. Zhang, M.M.F. Yuen, Enhanced conductivity induced by attractive capillary force in ternary conductive adhesive, Compos. Sci. Technol. 137 (2016) 109–117, https://doi.org/10.1016/j.compscitech.2016.10.028.

[30] H. Sun, M.M.F. Yuen, Conductivity enhancement of thermal interface material via capillary attraction, in: 2016 IEEE 66th Electronic Components and Technology Conference (ECTC), 2016, pp. 1409–1414, https://doi.org/10.1109/ECTC.2016.94.

[31] H. Sun, Z. Han, N. Willenbacher, Ultrastretchable conductive elastomers with a low percolation threshold for printed soft electronics, ACS Appl. Mater. Interfaces 11 (2019) 38092–38102, https://doi.org/10.1021/acsami.9b11071.

[32] S. Bindgen, J. Allard, E. Koos, The behavior of capillary suspensions at diverse length scales: from single capillary bridges to bulk, Curr. Opin. Colloid Interface Sci. 58 (2022) 101557, https://doi.org/10.1016/j.cocis.2021.101557.

[33] R. Xing, J. Yang, D. Zhang, W. Gong, T.V. Neumann, M. Wang, R. Huang, J. Kong, W. Qi, M.D. Dickey, Metallic gels for conductive 3D and 4D printing, Matter 6 (2023) 2248–2262, https://doi.org/10.1016/j.matt.2023.06.015.

[34] G. Schramm, Rheology 2 A Practical Approach to Rheology and Rheometry, 2000.

[35] M.I. Devoto, T. Timofte, A. Halm, D. Tune, Improved measurement of the contact resistivity of ECA-based joints. https://doi.org/10.4229/EUPVSEC20212021-1-4BO.5.6, 2021.

[36] ASTM International, Standard test method for apparent shear strength of single-lap-joint adhesively bonded metal specimens by tension loading (Metal-to- metal). https://doi.org/10.1520/D1002-10R19, 2010.

[37] N. Abdel Latif, R. Lamsairhri, T. Rößler, Characterization of mechanical strength of shingle joints using die shear tests, SiliconPV Conf Proc 1 (2024), https://doi.org/10.52825/siliconpv.v1i.944.

[38] G. Divitini, S. Cacovich, F. Matteocci, L. Cinà, A. Di Carlo, C. Ducati, In situ observation of heat-induced degradation of perovskite solar cells, Nat. Energy 1 (2016) 15012, https://doi.org/10.1038/nenergy.2015.12.

[39] T. Rößler, D. Von Kutzleben, N. Klasen, V. Nikitina, P. Baliozian, A. Münzer, E. Fokuhl, A. Kraft, Progress in shingle interconnection based on electrically conductive adhesives at Fraunhofer ISE, in: Bhubaneswar, India, 2022 020012, https://doi.org/10.1063/5.0127455.

[40] J. Weber, T. Roessler, How to assess the electrical quality of solar cell interconnection in shingle solar modules, Progr. Photovo. 31 (2023) 949–959, https://doi.org/10.1002/pip.3699.

[41] M.L. Clingerman, J.A. King, K.H. Schulz, J.D. Meyers, Evaluation of electrical conductivity models for conductive polymer composites, J. Appl. Polym. Sci. 83 (2002) 1341–1356, https://doi.org/10.1002/app.10014.

[42] D. Klosterman, L. Li, J.E. Morris, Materials characterization, conduction development, and curing effects on reliability of isotropically conductive adhesives, IEEE Trans. Compon. Packag. Manuf. Technol. 21 (1998). https://ieeexplore.ieee.org/stamp/stamp.jsp?tp=&arnumber=679028.

[43] F. Tan, X. Qiao, J. Chen, H. Wang, Effects of coupling agents on the properties of epoxy-based electrically conductive adhesives, Int. J. Adhesion Adhes. 26 (2006) 406–413, https://doi.org/10.1016/j.ijadhadh.2005.06.005.

[44] K. Tedjokusuma, W. Lauth, N. Willenbacher, Manufacture and filtration performance of glass filters made from capillary suspensions, Separ. Purif. Technol. 329 (2024) 125097, https://doi.org/10.1016/j.seppur.2023.125097.

[45] H. Sun, X. Zhang, M.M.F. Yuen, Enhanced conductivity induced by attractive capillary force in ternary conductive adhesive, Compos. Sci. Technol. 137 (2016) 109–117, https://doi.org/10.1016/j.compscitech.2016.10.028.

[46] C. Xu, N. Willenbacher, How rheological properties affect fine-line screen printing of pastes: a combined rheological and high-speed video imaging study, J. Coating Technol. Res. 15 (2018) 1401–1412, https://doi.org/10.1007/s11998-018-0091-2.

[47] S. Roh, D.P. Parekh, B. Bharti, S.D. Stoyanov, O.D. Velev, 3D printing by multiphase silicone/water capillary inks, Adv. Mater. 29 (2017) 1701554, https://doi.org/10.1002/adma.201701554.

[48] R. Aradhana, S. Mohanty, S.K. Nayak, A review on epoxy-based electrically conductive adhesives, Int. J. Adhesion Adhes. 99 (2020) 102596, https://doi.org/10.1016/j.ijadhadh.2020.102596.

[49] S.F. Ahmed, N. Islam, P.S. Kumar, A.T. Hoang, M. Mofijur, A. Inayat, G. M. Shafiullah, D.-V.N. Vo, I.A. Badruddin, S. Kamangar, Perovskite solar cells: thermal and chemical stability improvement, and economic analysis, Mater. Today Chem. 27 (2023) 101284, https://doi.org/10.1016/j.mtchem.2022.101284.

[50] G. Divitini, S. Cacovich, F. Matteocci, L. Cinà, A. Di Carlo, C. Ducati, In situ observation of heat-induced degradation of perovskite solar cells, Nat. Energy 1 (2016) 15012, https://doi.org/10.1038/nenergy.2015.12.

[51] T. Geipel, Electrically Conductive Adhesives for Photovoltaic Modules, Fraunhofer ISE, 2018. PhD Thesis.

[52] T.R. Klein, M.S. Young, A.C. Tamboli, E.L. Warren, Lamination of transparent conductive adhesives for tandem solar cell applications, J. Phys. Appl. Phys. 54 (2021) 184002, https://doi.org/10.1088/1361-6463/abe2c4.
[53] H.K. Kim, F.G. Shi, Electrical reliability of electrically conductive adhesive joints: dependence on curing condition and current density, Microelectron. J. 32 (2001) 315–321, https://doi.org/10.1016/S0026-2692(01)00007-6.
[54] T. Rößler, D. Von Kutzleben, N. Klasen, V. Nikitina, P. Baliozian, A. Münzer, E. Fokuhl, A. Kraft, Progress in shingle interconnection based on electrically conductive adhesives at Fraunhofer ISE, in: Bhubaneswar, India, 2022 020012, https://doi.org/10.1063/5.0127455.
[55] D. Jun, H. Son, J. Moon, S. Cho, S. hyun Kim, A study on correlation peel strength and the efficiency of shingled modules according to curing condition of electrically conductive adhesives, Curr. Photov. Res. 9 (2021) 31–35, https://doi.org/10.21218/CPR.2021.9.2.031.
[56] P. Gebhardt, G. Mülhöfer, A. Roth, D. Philipp, Statistical analysis of 12 years of standardized accelerated aging in photovoltaic-module certification tests, Progr. Photovo. 29 (2021) 1252–1261, https://doi.org/10.1002/pip.3450.